COBEM 2021 26th International Congress of Mechanical Engineering
November 22-26, 2021, Virtual Congress, Brazil

COB-2021-0988
COMSOL WITH MODIFIED NONLINEAR FUNCTION SPECIFICATION AND TEMPERATURE MOVING SENSOR TO ESTIMATE HEAT RATE IN A TIG WELDING PROCESS

Rodrigo Gustavo Dourado da Silva
Laboratório de Transferência de Calor – LabTC, Instituto de Engenharia Mecânica – IEM, Universidade Federal de Itajubá – UNIFEI, Campus Prof. José Rodrigues Seabra, Av. BPS, 1303, 37500-903, Itajubá, MG, Brazil.
rodrigogdourado@hotmail.com
Elisan dos Santos Magalhães
Instituto Tecnológico Aeronáutico – ITA, Divisão de Pós-Graduação e Pesquisa, Praça Mal, Eduardo Gomes, 50 – Vila das Acácias, 12228-900, São José dos Campos, SP, Brazil.
elisan@ita.br
Sandro Metrevelle Marcondes de Lima e Silva
Laboratório de Transferência de Calor – LabTC, Instituto de Engenharia Mecânica – IEM, Universidade Federal de Itajubá – UNIFEI, Campus Prof. José Rodrigues Seabra, Av. BPS, 1303, 37500-903, Itajubá, MG, Brazil.
metrevel@unifei.edu.br

Abstract. *The estimation of the imposed heat rate in welding processes has always been an obstacle to improve the thermal efficiency of these processes. Thus, the use of inverse problem techniques is an alternative procedure to estimate the heat rate. In this study, the problem is highly nonlinear; therefore, the heat flux provided by the welding process is estimated by the iterative Function Specification Method. This method was modified to estimate the heat supply based on the heat rate sensitivity coefficient, which represents the influence of the welding power in the temperatures of 304 stainless steel plates. In order to avoid the problem of low thermal sensitivity due to the movement of the welding source on the upper face of the plate, this methodology is based on the concept of temperature moving sensor. The software Comsol was used to solve the three-dimensional heat diffusion equation with enthalpy with phase change. The efficiency of the process was calculated with the estimated net heat rate which ranged from 63% to 87%. The average efficiency obtained was 75% for this welding process. A relation between the energy rate given by the power supply and the estimated efficiency was also observed.*

Keywords: *inverse heat conduction problem, TIG welding process, heat flux estimation, thermal efficiency, design of experiments.*

1. INTRODUCTION

Tungsten Inert Gas (TIG) welding is one of the most popular gas shielding arc welding process used in many industrial fields such as aerospace, automotive, nuclear, ship building and petrochemical industries where excellent joint quality is required. In this process, a tungsten electrode is protected by a flow of inert gas and the workpiece is joined by voltaic arc generated from a moving heat source and with the help of filler material. Despite the recent major advances in metal welding, it is still a difficult task to measure the heat flux delivered to the weld joint during the process. For example, the determination of the heat flux delivered to a plate during a TIG welding process can be performed by measuring the temperature in the fusion zone. However, due to the high thermal gradient and casting of the thermocouple with the weld, that possibility becomes unfeasible. So, inverse problem techniques may be used to estimate the amount of heat transferred during this process. The Inverse Heat Conduction Problem (IHCP) solution is typically obtained from optimization techniques. In optimization, the variable to be minimized must change in each iteration, so that the quantity measured in a given sample point approach the value obtained by the numerical model, and so, the iterative process converge. However, this estimation process is affected when the experimental temperature data present noise or when they have low sensitivity in relation to the parameter to be estimated, that is, when the rate of change of the experimental data relative to the parameter to be estimated is small. There are diverse techniques that are applied to inverse problem solutions. Some of them are described below.

The study and use of inverse problem techniques have been growing in recent years. Alifanov (1974) used the Conjugated Gradient technique with adjoint equation to estimate functions in IHCP. The method is based on an optimization process with iterative regularization. This technique can be used to solve linear and nonlinear problems to estimate functions or parameters. Tikhonov and Arsenin (1977) proposed a method that became known as Tikhonov Regularization, in which the Duhamel's theorem and an optimization by least squares is used, but a linear factor is added to regularize the noise present in the experimental temperatures. In Beck et al. (1985), the authors used the Duhamel's

theorem, Taylor series expansion and optimization by least squares to develop the linear Function Specification method. This method presents robustness to noise present in the data, is easy to implement and does not require long processing time. Later, the Function Specification method was developed to work with nonlinear problem, as presented in Woodbury (2003). Some authors used filters for the solution of inverse problems in heat transfer. In this case, Kalman filters and Dynamic Observers can be cited, for example, Tuan et al. (1996), Lee et al. (2000), Park and Jung (2000). These methods are based on the theory of dynamic and control systems and have been used in real-time reconstruction of unknown variables of the system, as for example, unknown boundary conditions.

New techniques of inverse problems have been developed, as for example, in Najafi and Woodbur (2015). An Artificial Neural Network (ANN) was used as a digital filter to estimate the heat flux almost in real time by using temperature data. By considering the temperatures as the input and heat flux as the output, the weights were interpreted as filter coefficients. The developed method was tested in several cases by using exact solutions and numerical models. Li et al. (2017) developed a Modified Space Marching method to solve the inverse problem in transient and nonlinear heat conduction problems combined with the Function Specification method. Future temperature measurements are used in a least square manner to stabilize the calculation results. Transient surface temperature and heat flux can be accurately recovered by the method without the need to employ the iteration procedure or the data smoothing technique. Magalhães et al. (20188) developed an inverse problem technique called Time Traveling Regularization (TTR) which has a modification based on the concept of time travel.

Many authors have used some of the inverse problem techniques aforementioned to estimate the amount of heat in welding processes. For example, Dal et al. (2012) modeled a TIG welding process using the Conjugate Gradient method with adjoint equation. The goal of that work was to apply an Arbitrary Lagrangian Eulerian (ALE) moving mesh method suitable to solve two-dimensional and axisymmetric moving-boundary problems. In order to calculate the fluid flow inside the fusion zone, the authors made simplifications: the fusion area was calculated by an analytic equation and the shape was estimated by an inverse method. Gonçalves et al. (2010) studied an inverse problem applied to the TIG welding process. In that work, the non-regularized Golden Section method was used to solve an inverse problem of entire domain. Although the Golden Section method is good to estimate parameters in nonlinear problems, it does require many iterative calculations increasing the computational cost. In addition, the heat flux is time dependent and it is best represented if estimated sequentially. Dal et al. (2014) used the inverse heat conduction problem to estimate the geometry of the weld pool in relation to time in a TIG process using the commercial software COMSOL Multiphysics coupled with a code in Matlab. In this problem, the heat source was assumed to be stationary in a solid 2D axisymmetric domain. An inverse methodology based on the TTR was proposed by Magalhães et al. (2018) to estimate the temporal heat input distribution in a TIG welding process. A numerical temperature moving sensor was also proposed to allow the temporal heat input estimation. It is a cheaper and more precise way to determine the heat input during a welding process.

In this paper, a methodology to estimate the heat supply in a welding process using an inverse problem approach is proposed. To achieve this purpose, experiments were performed on a 304 stainless steel plate in the TIG welding process. The direct heat transfer problem was modeled using the three-dimensional nonlinear heat diffusion equation with phase change, where the mushy zone between solid and liquid phases was considered. The moving heat source provided by the arc was modeled using a Gaussian function. The heat conduction direct problem was calculated by a Finite Element method, using the software COMSOL. The inverse problem was solved by a code developed in Matlab, which communicates with COMSOL through a LiveLink feature.

2. THEORETICAL DEVELOPMENT

2.1 Direct problem

Figure 1 presents a simplified model for a welding process. The heat rate, $q(t)$, provided by the TIG Welding torch, is delivered within the moving circular region. The weld bead has a width of L_W. The plate loses heat by convection in the room, so $h(T)$ is the heat transfer coefficient. Heat radiation emitted by the plate to the surroundings is also considered, so $\varepsilon(T)$ is the emissivity (Magalhães *et al.*, 2018).

The thermal model presented in Figure 1 may be described by the transient three-dimensional diffusion equation with phase change problem:

$$\frac{\partial}{\partial x}\left(k(T)\frac{\partial T}{\partial x}\right)+\frac{\partial}{\partial y}\left(k(T)\frac{\partial T}{\partial y}\right)+\frac{\partial}{\partial z}\left(k(T)\frac{\partial T}{\partial z}\right)=\rho\frac{\partial H(T)}{\partial t} \tag{1}$$

where k is the nonlinear thermal conductivity, T is the temperature, x, y, and z the cartesian coordinates, t is the time, ρ is the density, and H is the enthalpy function. H is defined as:

$$H=\int C_p\,dT+(1-\theta)L \tag{2}$$

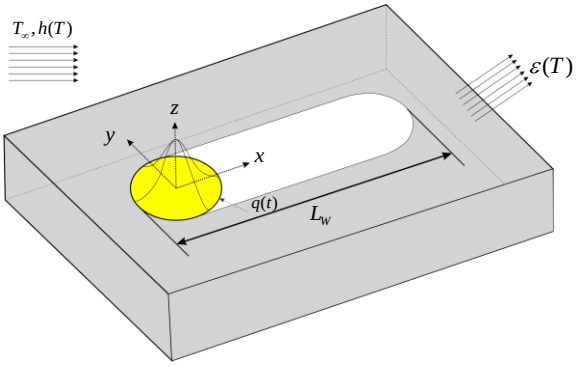

Figure 1. Representation of the thermal model in TIG process.

where L is the latent fusion heat, C_p is the specific heat and θ is a function defined as:

$$\theta(T)=\begin{cases}1 & T \le T_m - \Delta T/2 \\ 1-\dfrac{T-T_m+\dfrac{\Delta T}{2}}{\Delta T} & T_m-\dfrac{\Delta T}{2} < T < T_m+\dfrac{\Delta T}{2} \\ 0 & T \le T_m + \Delta T/2\end{cases} \tag{3}$$

where T_m is the fusion temperature and ΔT is the temperature interval of transition between solid and liquid phases.

The boundary conditions of convection and radiation are considered on all surfaces:

$$-k(T)\frac{\partial T}{\partial \eta_i} = h(T)(T-T_\infty)+\sigma\varepsilon(T)(T^4-T_\infty^4) \tag{4}$$

where i is an index for the surface, η is the normal coordinate, σ is the Stefan-Boltzmann constant, and T_∞ is the room temperature.

The boundary condition of prescribed heat flux is considered in the circular area, Figure 1:

$$-k(T)\frac{\partial T}{\partial z} = q(x,y,t) \tag{5}$$

The heat flux was distributed according to the Gaussian radial model expressed by Goldak and Akhlaghi (2005) as follows:

$$q(x,y,t)=\frac{3Q(t)}{\pi \times r_s^2} e^{-3\frac{(x-u)^2}{r_s^2}} e^{-\frac{3y^2}{r_s^2}} \tag{6}$$

where Q is the applied heat rate, r_s is the radius of the circular region of Figure 1 and u is the welding velocity.

The initial condition adopted:

$$T(x,y,z,0)=T_0 \tag{7}$$

where T_0 is the initial temperature at the instant 0.

2.2 Temperature moving sensor

Consider a moving heat source with speed u in direction x, as shown in Figure 2. The heat source starts its movement in the coordinates (x_1, y_0) and advances in spacing $\Delta x = u\Delta t$ up to position (x_n, y_0), in which Δt is the computational time step. In this way a vector of positions can be defined, as x given by:

$$\boldsymbol{x} = \begin{bmatrix} x_1 \\ x_2 \\ \vdots \\ x_n \end{bmatrix} \tag{8}$$

$$x_j = x_1 + (j-1)u\Delta t$$
$$j = 2,\ldots,n \tag{9}$$

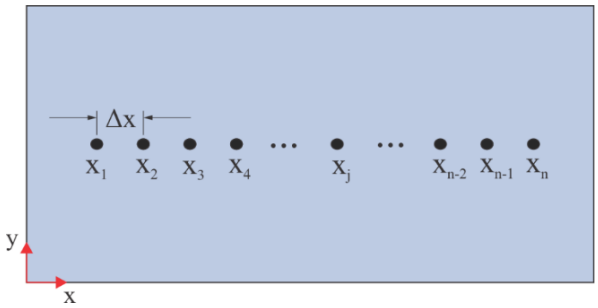

Figure 2. Positions x_j along the metal plate.

where n is the total number of time steps. Similarly, vector t is defined, which represents the time discretization. Temperature vector, T_{ms}, represent the moving sensor and it is defined as:

$$\boldsymbol{T_{ms}} = \begin{bmatrix} T_1 \\ T_2 \\ \vdots \\ T_n \end{bmatrix} \tag{10}$$

$$T_i = T(x_i, t_i)\,,\ i = 1,\ldots,n \tag{11}$$

The purpose of the Temperature Moving Sensor is to represent a fictitious sensor that moves along with the heat source to avoid problems of thermal sensitivity. Such problems arise when the heat source moves away from the point of temperature measuring, causing a sharp drop in the sensitivity coefficient value which may cause inaccuracy in the heat flux estimation. Therefore, when using the moving sensor, the sensitivity coefficients will remain stable thus improving the accuracy of the estimated function and decreasing computational cost due a high convergence rate.

The Temperature Moving Sensor is obtained through the measured temperatures on the opposite surface of the plate aligned with the heat source direction. Afterwards, a computational code is used to better interpolate the measured data, as shown in Figure 3. Notice that in this example, the fifth thermocouple is disregarded, since its data is statistically far from the others. In the case of the TIG Welding process discussed in this paper, the moving sensor moves in a straight line on the opposite surface of the plate. In other cases, where the heat source has a curved trajectory, the same method can be used, since this trajectory can be parameterized in relation to time.

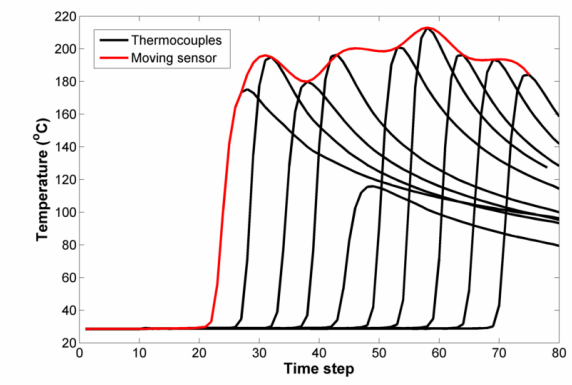

Figure 3. Example of a temperature moving sensor.

2.3 Estimation of the gaussian heat flux

In Equation (6), it may be noticed that the heat rate, $Q(t)$, supplied by the welding process, is the only parameter that contributes to change the Gaussian Function, once all the other parameters that define the heat flux boundary region are constants in relation to time. Thus, the temperature variation in a specific position in the domain depends only on $Q(t)$.

The power sensitivity coefficient, Z, represents the sensitivity of temperature at position $p=(x,y,z)$ in relation to changes on the parameter $Q(t)$ and is defined by

$$Z(\boldsymbol{p},t)=\frac{\partial T(\boldsymbol{p},t)}{\partial Q(t)} \tag{12}$$

Using the same concept of section 2.2, the moving sensitivity coefficient, Z_{ms}, which follows the same movement of the heat source, is defined.

$$\boldsymbol{Z}_{\boldsymbol{ms}}=\begin{bmatrix} Z_1 \\ Z_2 \\ \vdots \\ Z_n \end{bmatrix} \tag{13}$$

A common method to calculate the sensitivity coefficient is to approximate the derivative by a quotient of differences (Beck *et al.*, 1985). Thus, considering $\boldsymbol{\delta} \ll \mathbf{1}$, the approximate value of Z_{ms} is given by:

$$\boldsymbol{Z}_{\boldsymbol{ms}}=\frac{\boldsymbol{T}_{\boldsymbol{ms}}[(1+\delta)Q(t_i)]-\boldsymbol{T}_{\boldsymbol{ms}}[Q(t_i)]}{\delta Q(t_i)} \tag{14}$$

The criterion used to estimate the Gaussian heat flux boundary condition is the minimization of a sum of squares between the measured temperatures, $Y_{ms,}$ and the calculated temperatures, T_{ms}, given by Eq. (15). For this purpose, the Gauss minimization method is used. In this method the calculated temperatures are approximated by first-order Taylor series.

$$S_M=(\boldsymbol{Y}_{\boldsymbol{ms}_M}-\boldsymbol{T}_{\boldsymbol{ms}_M})^T(\boldsymbol{Y}_{\boldsymbol{ms}_M}-\boldsymbol{T}_{\boldsymbol{ms}_M}) \tag{15}$$

In Equation (15), the index M, represents the current time step of heat flux estimation. The regularization method for this inverse problem is accomplished by the future time steps technique proposed by Beck et al. (1985). The future time steps regularization uses temperature information of r time steps ahead of the present time M to estimate the heat flux. Thus, vectors $\boldsymbol{Y}_{\boldsymbol{ms}_M}$ and $\boldsymbol{T}_{\boldsymbol{ms}_M}$ are defined by Eq. (16).

$$\boldsymbol{Y}_{\boldsymbol{ms}_M}=\begin{bmatrix} Y_M \\ Y_{M+1} \\ \vdots \\ Y_{M+r-1} \end{bmatrix}, \quad \boldsymbol{T}_{\boldsymbol{ms}_M}=\begin{bmatrix} T_M \\ T_{M+1} \\ \vdots \\ T_{M+r-1} \end{bmatrix} \tag{16}$$

The first-order Taylor expansion of temperature T_{ms} in relation to the heat rate results in:

$$\boldsymbol{T}_{\boldsymbol{ms}}\big|_{Q+\Delta Q}=\boldsymbol{T}_{\boldsymbol{ms}}\big|_{Q}+\left.\frac{\partial \boldsymbol{T}_{\boldsymbol{ms}}}{\partial Q}\right|_{Q}\Delta Q=\boldsymbol{T}_{\boldsymbol{ms}}\big|_{Q}+\boldsymbol{Z}_{\boldsymbol{ms}}\big|_{Q}\Delta Q \tag{17}$$

By substituting Eq. (17) into Eq. (15) and minimizing it to ΔQ, an expression to calculate the heat rate increment is obtained (Eq. 18). This value is used to calculate the heat rate at time M by the iterative procedure given in Eq. (19).

$$\Delta Q=\left(\boldsymbol{Z}_{\boldsymbol{ms}_M}{}^T\boldsymbol{Z}_{\boldsymbol{ms}_M}\right)^{-1}\boldsymbol{Z}_{\boldsymbol{ms}_M}{}^T\left(\boldsymbol{Y}_{\boldsymbol{ms}_M}-\boldsymbol{T}_{\boldsymbol{ms}_M}\right) \tag{18}$$

$$Q_M{}^{k+1}=Q_M{}^k+\Delta Q^k \tag{19}$$

Index k in Eq. (19) represents the iterative procedure. According to Woodbury (2003), the convergence criterion sometimes is hard to obtain. In this way, it is assumed that the convergence is satisfied if the relative error is lower than the tolerance τ established, as shown in Eq. (20).

$$\frac{\Delta Q^k}{Q_M{}^k} < \tau \tag{20}$$

Finally, considering $Q_M{}^*$ as the estimated heat rate at time step M, the Gaussian heat flux distribution at time t_M, is given by Eq. (21).

$$q(x, y, t_M) = \frac{3Q_M{}^*}{\pi r_s^2} e^{-3\frac{(x-x_M)^2}{c^2}} e^{-3\frac{y^2}{c^2}} \tag{21}$$

3. NUMERICAL MODEL

The direct problem described in Section 2 was solved by using COMSOL 5.3a software. Table 1 shows the parameter values of the thermal model.

Table 1. Parameters of the thermal model.

Parameter	Value	Description
u	50 cm/min	Welding velocity
r_s	1.8 mm	Heat input radius
Δt	0.38 s	Time interval
T_m	1400 ºC	Fusion temperature
L	265200 J/kg	Latent heat of fusion
ρ	7900 kg/m³	Density
ΔT	80 K	Temperature range of mushy zone

The thermal conductivity, k [W/(mºC)], and the specific heat at constant pressure, C_p [J/(kgºC)], of the AISI 304 stainless steel used in the numerical thermal model are defined by Eqs. (22-23) (Park and Jung, 2000). In the mushy zone, it was considered that the thermal properties vary linearly according to the solid-liquid fraction θ.

$$k = \begin{cases} 14.30 + 0.01983T - 5.451\times10^{-6}T^2 & \theta = 1 \\ k = \theta k\big|_{T_m - \Delta T/2} + (1-\theta)k\big|_{\theta=0} & 0 < \theta < 1 \\ 31.378 & \theta = 0 \end{cases} \tag{22}$$

$$C_p = \begin{cases} 460.5 + 0.4257T - 5.050\times10^{-4}T^2 + 2.6608\times10^{-7}T^3 & \theta = 1 \\ \theta C_p\big|_{T_m - \Delta T/2} + (1-\theta)C_p\big|_{\theta=0} & 0 < \theta < 1 \\ 796.584 & \theta = 0 \end{cases} \tag{23}$$

4. EXPERIMENTAL PROCEDURE

In this work, a 200mm × 50mm × 4 mm AISI 304 stainless steel plate bearing ten type K thermocouples attached by capacitive discharge on the surface opposite to the heated one. Nine TIG welding experiments were performed in order to verify the obtained temperature for a set of 9 experimental conditions. More details on the thermocouple positioning may be seen in Magalhães et al. (2018). The welding velocity was fixed at 50 cm/min and the welding parameters for each experiment are shown in Table 2.

Table 2. Welding parameters.

Sample	Room temperature [ºC]	Arc length [mm]	Electrode tip angle [º]	Shielding gas	Current [A]
E1	28.88	2	30	Air	41
E2	28.84	3	30	Air+25% He	70
E3	28.56	4	30	Air+25% He	101
E4	36.89	2	60	Air+25% He	70
E5	27.85	3	60	Air	101
E6	28.63	4	60	Air+25% He	41
E7	29.98	2	90	Air+25% He	101
E8	30.05	3	90	Air+25% He	41
E9	29.67	4	90	Air	70

5. RESULTS AND DISCUSSION

The heat flux was estimated for the nine experiments listed in Section 4. In addition, the thermal efficiency of each welding process was calculated, and the optimal welding parameters were estimated by statistical method.

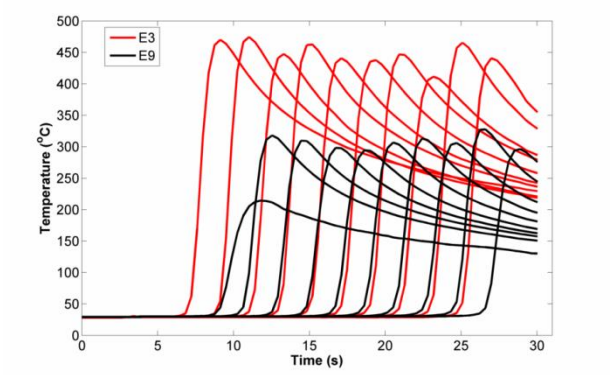

Figure 4. Measured temperatures of experiments E3 and E9.

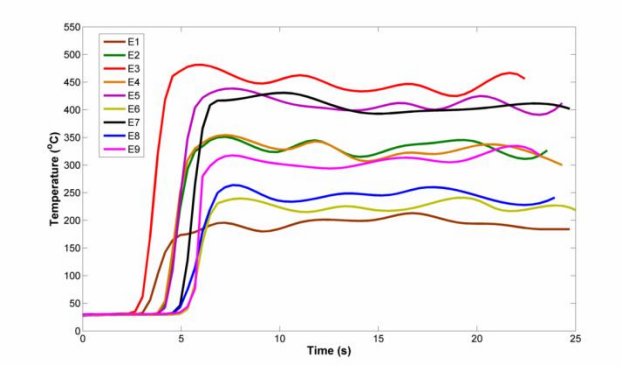

Figure 5. Calculated Temperature Moving Sensors.

Figure 4 shows the temperatures measured by 10 thermocouples located on the lower surface of the steel plate of experiments E3 and E9. The Temperature Moving Sensors calculated from the experimental temperatures, Y_{ms}, for all nine experiments are shown in Figure 5. These curves are obtained by the interpolation of the measured temperatures for each experiment.

Figure 6 shows the estimated heat rate in relation to time, $Q(t)$, delivered to the stainless steel plate AISI 304 in the nine experiments. By using the estimated values, the average heat rate was calculated, as well as the respective welding thermal efficiency (Table 4). The heat rate in the welding process showed an average constant behavior, making the convergence process easier. After the initial seconds of heating, the convergence was achieved with only two iterations, in average, for each time step, reaching a relative error in the order of 10^{-09}, as shown in Figure 7. The computational time ranged from 440 minutes (E1) to 800 minutes (E3) using an Intel Core i7 - 4790 -.3.6 GHz processor.

A comparison between the estimated and the experimental temperatures for experiment E9 is presented in Figure 8. Notice that the behavior of the estimated temperatures matches the measured ones, presenting an average difference of 4.3% at the maximum values. The same behavior is obtained for the other experiments (Tab. 4). It is important to note that the theoretical model seeks to represent the physical phenomena as much as possible, but it is still difficult to find the exact parameters and properties in literature, which may cause divergences between the numerical models and experimental results.

Notice a correlation between the thermal efficiency and the welding power supplied by the process. The higher the imposed heat rate, the lower the thermal efficiency of the welding process, as shown in Figure 9. The red line in this figure represents a quadratic data fitting given by Eq. (24) for the heat range analysed and has coefficient of determination of 83%.

$$\eta(Q) = 120 - 0.12Q + 7.1\times10^{-5}Q^2, \quad 293 < Q < 685 \tag{24}$$

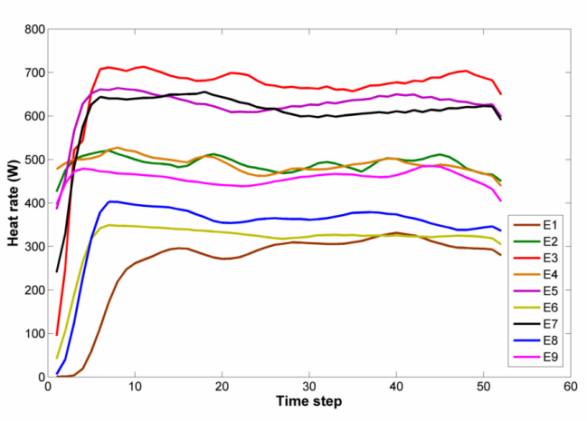

Figure 6. Estimated heat rate in relation to time.

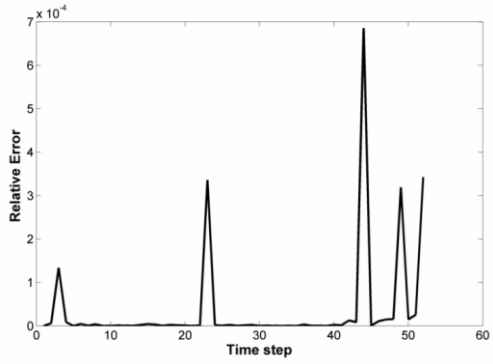

Figure 7. Convergence plot for E9.

Table 3. Average estimated thermal efficiency

Sample	Average estimated heat rate [W]	Average thermal efficiency [%]
E1	293.33	87.2
E2	491.46	70.6
E3	684.58	63.4
E4	491.09	76.9
E5	635.32	65.5
E6	329.75	77.8
E7	623.22	72.6
E8	369.67	86.7
E9	461.07	67.9

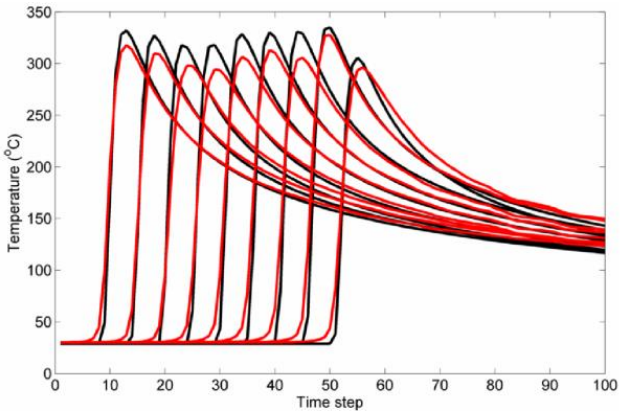

Figure 8. Numerical (black) and experimental (red) temperatures in experiment E9.

where η is the thermal efficiency.

In literature, it is possible to find thermal efficiency values in the range of 21% to 90% for all types of materials and welding parameters. For the TIG welding process performed in this work, the average thermal efficiency is 75%. This value is consistent with the recent work on this topic. According to Stenbacka (2013), based on TIG studies for the stainless steel 304, over the last two decades, the average experimental thermal efficiency is in the range of 56% to 85%.

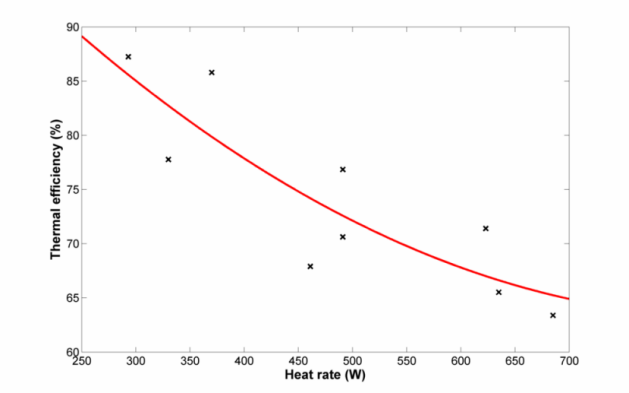

Figure 9. Relation between the heat input rate and thermal efficiency.

In order to investigate the influence of the welding parameters on the thermal efficiency for this problem, the Taguchi method was used. The electrode type, arc length, shielding gas and welding current were analyzed at the established levels in Table 3. As shown in Figure 10, the current is statistically significant to determine the efficiency with a level of significance of 10%. Thus, the lower the current (and hence the welding power), the higher the thermal efficiency for this process. This behavior is also mentioned in the experimental work by Rykalin (1951), Niles and Jackson (1975) and Dutta et al. (1994) on TIG.

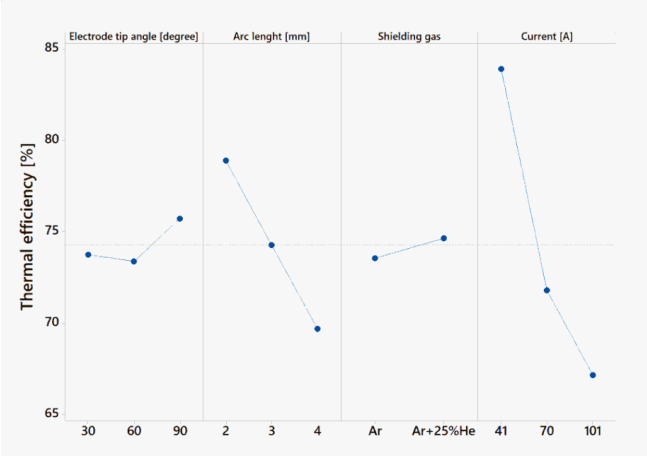

Figure 10. Influence of welding parameters on thermal efficiency analyzed by Taguchi method.

The arc length also has statistical relevance in relation to the thermal efficiency. Notice that the larger the distance between the electrode and the plate, the lower the thermal efficiency, since long arcs lose more energy to the environment. This behavior is also observed in the work by Rykalin (1957), Ghent et al. (1979) and Collings et al. (1979).

The electrode tip angle and the shielding gas showed no significant influence, although the increase in He concentration is related to an increase in thermal efficiency (Figure 10). Results on thermal efficiency obtained by Niles and Jackson (1975) and Smartt (1990) showed that for five different ratios of He, the shielding gas has little or no influence on the thermal efficiency of 304 stainless steel. For Collings et al. (1979), changes in the electrode tip angle has also no significance in the variation of the thermal efficiency.

6. CONCLUSION

In this paper, the effective heat rate in a TIG welding process was estimated. A nonlinear heat conduction problem with phase changing was considered in which the thermal properties vary linearly in the mushy zone. The commercial software COMSOL was used to solve the direct problem matched with an inverse problem code in Matlab. The developed code to solve the inverse problem uses the Gauss optimization method with future time steps regularization to estimate the heat rate.

It was noticed that the Temperature Moving Sensor ensured good thermal sensitivities to estimate the heat rate. The estimated heat rates for all nine experiments showed an approximately constant behavior during welding. The welding average thermal efficiency obtained for the TIG process in this work was 75%. In addition, a correlation between the

welding power and the thermal efficiency was statistically confirmed. Through Taguchi analysis, it was noted that the current and the arc length significantly influence the thermal efficiency. The shielding gas and the electrode tip have no significant effect on the process studied in this work.

This methodology presents a fast and cheap way to study TIG welding process showing that the thermal efficiency drops with the increase of the power supply.

7. ACKNOWLEDGEMENTS

The authors would like to thank CNPq, CAPES and FAPEMIG for their financial support.

8. REFERENCES

Alifanov, O. M., 1974. Solution of an inverse problem of heat conduction by iteration methods, Journal of Engineering Physics, 26, 471-476.

Assael, M. J., Gialou, K., 2003. Measurement of the thermal conductivity of stainless steel 304L up to 550 K, International Journal of Thermophysics, 24, 1145-1153.

Beck, J.V., Blackwell, B. and Clair, C., 1985. Inverse heat conduction: ill-posed problems, Wiley-Interscience Publication.

Collings, N., Wong, K.Y., Guile, A.E., 1979. Efficiency of tungsten-inert-gas arcs in very-high-speed welding, Proc. IEE, 126, 276 – 280.

Dal, M., Le Masson, P., Carin, M., 2014. A model comparison to predict heat transfer during spot GTA welding, International Journal of Thermal Sciences, 75, 54–64.

Dal, M., Le Masson, P., Carin, M., 2012. Estimation of fusion front in 2D axisymmetric welding using inverse method, International Journal of Thermal Sciences, 55, 60-68.

Dutta, P., Joshi, Y., Franche, C., 1994. Determination of gas tungsten arc welding efficiencies. Experimental Thermal and Fluid Science, 9, 80-89.

Ghent, H. W. , Roberts, D.W., Hermance, C.E., Kerr, H.W, Strong, A.B., 1979. Arc efficiencies in TIG welds, Conf. Proc. Arc physics and weld pool behavior, The Welding Institute.

Goldak, J.A., Akhlaghi, M., 2005. Computational welding mechanics, Springer, USA.

Gonçalves, C.V. , Carvalho, S.R., Guimarães, G., 2010. Application of optimization techniques and the enthalpy method to solve a 3D-inverse problem during a TIG welding process, Applied Thermal Engineering, 30, 2396-2402.

Holman, J. P., 2001. Experimental methods for engineers, 7th ed., McGraw-Hill Book Company, New York.

Lee, W. -S., Ko, Y. -H., Ji, C. -C., 2000. Study of an inverse method for the estimation of impulsive heat flux, Journal of the Franklin Institute, 337, 661-671.

Li, R., Huang, Z., Li, G., Wu, X., Yan, P., 2017. A modified space marching method using future temperature measurements for transient nonlinear inverse heat conduction problem, International Journal of Heat and Mass Transfer, 106, 1157-1163.

Magalhães, E. S., Anselmo, B. C. S, Lima e Silva, A. L. F., Lima e Silva, S. M. M., 2018. Time traveling regularization for inverse heat transfer problems, Energies, 11, 507-521.

Magalhães, E. S., Lima e Silva, A. L. F., Lima e Silva, S. M. M., 2018. A thermal efficiency analysis of a gas tungsten arch welding process using a temperature moving sensor, International Journal of Thermal Sciences, 129, 47-55.

Najafi, H., Woodbury, K. A., 2015. Online heat flux estimation using artificial neural network as a digital filter approach, International Journal of Heat and Mass Transfer, 91, 808-817.

Niles, R. W., Jackson, C. E. , 1975. Weld thermal efficiency of the GTAW process, Welding Journal, 54, 26s-32s.

Park, H. M., Jung, W. S., 2000. A recursive algorithm for multidimensional inverse heat conduction problems by means of mode reduction, Chem. Eng. Sci., 55, 5115–5124.

Rykalin, N. N., 1951. Calculation of heat flow in welding (translated by Z. Paley and C. M. Adams, Jr. Trans.).

Rykalin, N. N., 1979. Berechnung Der Wärmevorgänge Beim Schweissen, VEB Verlag Technik, Berlin.

Smartt, H. B., 1990. Arc-welding processes, Materials Processing: Theory and Practices, 175–208.

Stenbacka, N., 2013. On arc efficiency in gas tungsten arc welding, Soldagem & Inspeção, 18, 380-390.

Taylor, J. R., 1997. An introduction to error analysis: the study of uncertainties in physical measurements, University Science Books, USA.

Tikhonov, A. N., Arsenin, V. Y., 1977. Solutions of ill-posed problems, V. H. Winstons and Songs, Washington, DC.

Tuan, C. , Ji, C.-C., Fong, L. -W. and Huang, W.-T., 1996. An input estimation approach to on-line two-dimensional inverse heat conduction problems, Numerical Heat Transfer Part B, 29, 345-363.

Woodbury, K. A., 2003. Inverse engineering handbook, CRC Press, Boca Raton.

9. RESPONSIBILITY NOTICE

The authors are the only responsible for the printed material included in this paper.